Quantum-size effects in ultrathin Ag films on V(001): Electronic structure and photoelectron spectroscopy

A. Ernst and J. Henk*
Max-Planck-Institut für Mikrostrukturphysik, Weinberg 2, D-06120 Halle (Saale), Germany

M. Lüders
International School for Advanced Studies (SISSA), 34014 Trieste, Italy

Z. Szotek and W. M. Temmerman
Daresbury Laboratory, Warrington WA4 4AD, United Kingdom
(Received 1 July 2002; published 30 October 2002)

First-principles calculations are performed to investigate in detail the electronic structure of ultrathin Ag films deposited on V(001). Quantum-well states in the Ag films show the typical dispersion with film thickness, but their spectral densities differ significantly from those of model systems. *Ab initio* calculations for several systems (bulk, surfaces, interfaces, and thin films) reveal as origins band-structure effects and hybridization between Ag and V states. Quantization effects show up as intensity oscillations in the constant-initial-state mode of photoelectron spectroscopy. Earlier experimental investigations, which reported inconsistencies with typical manifestations of quantization effects, are discussed.

DOI: 10.1103/PhysRevB.66.165435 PACS number(s): 73.20.At, 73.21.Fg, 79.60.Dp

I. INTRODUCTION

Quantum-well (QW) states play an important role in many aspects of condensed matter physics; to name just two, interlayer exchange coupling[1,2] and the onset of magnetism in ultrathin films[3,4] (experimentally, a quantum well is realized as a film grown on a substrate). Their properties are therefore investigated both experimentally and theoretically with great effort and success. Theoretically, basic properties of spatially confined electrons can be obtained by model calculations that are based either on the free-electron picture[5] or on tight-binding models[6,7] (for books and reviews, see Refs. 8–11). In particular, tight-binding models revealed and explained manifestations of the electron's spatial confinement in angle-resolved photoelectron spectroscopy (PES): a weakening of the wave vector conservation with decreasing film thickness, and pronounced oscillations with film thickness and with photon energy (for experiments, see Refs. 12–15).[7] For prototypical systems such as Cu/Co(001), Co/Cu(001), and Ag/Fe(001) (for selected publications, see Refs. 16–23), the ''fingerprints'' of QW states could be well observed and the experimental findings could almost perfectly be explained by model calculations.

Whereas surfaces and films of late transition metals (TM's) (e.g., Fe, Co, Ni, Ru, Rh, and Pd) and of noble metals (e.g., Cu, Ag, and Au) are well understood, the early TM's (e.g., V, Cr, and W) show a more unexpected and less understood behavior. For example, theoretical calculations predicted a magnetic V(001) surface, depending on the underlying assumptions (e.g., surface-layer relaxation and exchange-correlation potential; see, for example, Refs. 24–27; for experiments, see Ref. 28). Further, surface alloys of early and late TM's can become magnetic, although their bulk and surfaces are not.[29] Silver films on V(001) are particularly interesting systems concerning electron-phonon coupling[30] and thin-film magnetism.[31,32] A violation of Hund's third rule was recently reported for thin W layers in Fe/W multilayers.[33] These are only a few indications that surfaces of early TM's behave rather differently as compared to late TMs. Hence it was not too surprising that recent PES experiments on QW states in Ag/V(001) found features in the spectra that could not be explained by model calculations.[34–36] That is, intensity oscillations with photon energier of some of the QW states behaved differently than expected.

We performed a detailed theoretical investigation to understand the properties of Ag films on V(001), the results of which are presented in this paper. Based on first-principles calculations, the paper addresses both electronic structure and photoemission, the latter with the aim to understand the aforementioned PES experiments. This paper is organized as follows. Computational aspects are addressed in Sec. II. Subsequently, the results of the electronic structure (Sec. III A) and the photoemission calculations (Sec. III B) are presented and discussed. Concluding remarks are given in Sec. IV.

II. COMPUTATIONAL ASPECTS

A. *Ab initio* calculations

The results presented in the forthcoming sections were obtained within the frameworks of the scalar-relativistic linearized-muffin-tin-orbital (LMTO) and layer-Korringa-Kohn-Rostoker (LKKR) methods. Self-consistent calculations were performed for bulk systems, semi-infinite systems [Ag(001), V(001) covered by up to 10 ML of Ag], and a Ag(001)/V(001) interface. We applied the local-density approximation with von Barth-Hedin[37] (LMTO) and Perdew-Wang[38] (LKKR) exchange-correlation potentials of density-functional theory. The bulk-band structures $E(\vec{k})$ of Ag and V (by the LMTO) method as well as spectral densities (SDs, by the LKKR method) resolved with respect to

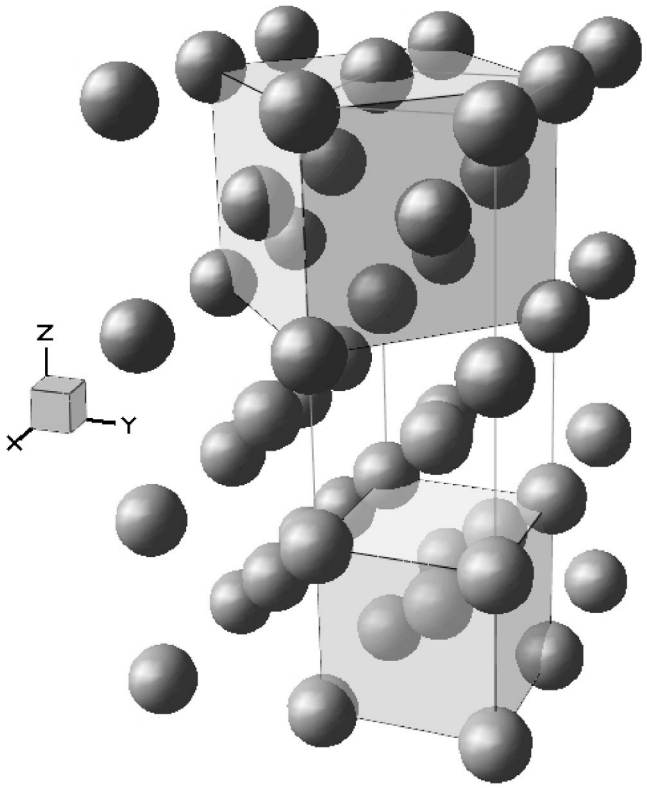

FIG. 1. Schematic geometry of 3 ML Ag on V(001). Vanadium (light gray, bottom) forms a bcc lattice, whereas silver (dark gray, top) grows pseudomorphically but tetragonally distorted on V. The fct unit cell of Ag is rotated by 45° with respect to the V lattice (cf. the transparent polyhedra). The *X*, *Y*, and *Z* axes are along the [100], [010], and [001] directions of the V lattice, respectively.

layer, in-plane wave vector $\vec{k}_{\parallel}$, and group representation were computed for the characterization of the electronic structures. The maximum angular momentum chosen was $l_{\max}=3$. More details on our computational method can be found in Refs. 39 and 40.

For all systems studied in this paper, vanadium layers are labeled by seminegative integers $(-\infty, \ldots, -2, -1, 0)$, the outermost surface or interface layer with index 0 and a bulk layer with index $-\infty$. Silver layers are indexed by positive integers, with a bulk layer labeled ∞. To be in agreement with previous works on surfaces, the conventional nomenclature *S*, *S*−1, *S*−2, etc., for surface layers and *B* for bulk layers is given in addition.

Vanadium occurs in a body-centered-cubic (bcc) lattice with first-nearest-neighbor distance of $5.707a_0$ (Bohr radii), whereas Ag crystallizes in a face-centered-cubic (fcc) lattice with 1NN distance of $5.465a_0$. Silver grows pseudomorphically on V, i.e., the first Ag layer occupies bcc sites (Fig. 1).[34] Therefore, the Ag-Ag distance has to be increased by 4.2% with respect to its bulk value. This in-plane stretching results in a reduced interlayer distance, i.e., a face-centered-tetragonal (fct) distortion, because the volume of the three-dimensional unit cell of Ag is conserved to a first approximation. We assumed that the distances between all V layers were given by the bulk value of $2.854a_0$. For all thicknesses of the Ag films, the distance from the last V layer (with label 0) to the first Ag layer (label 1) was $3.289a_0$, that between the first and the second Ag layer (label 2) $3.667a_0$, and those between all subsequent Ag layer $3.701a_0$ (the fcc bulk value $3.864a_0$).[34] Our choice of Wigner-Seitz radii reflected these structural aspects. That is, we took $2.88a_0$ for the V radii at the interface, and $2.81a_0$ in all other layers. The Ag radii varied from $3.00a_0$ at the interface to $3.06a_0$ in the bulk.

Quantum-well states in the Ag film were identified with help of the spectral densities (SD's). These states show sizable spectral weight in the whole film and decreasing weight towards the bulk. In contrast, surface (interface) states exhibit a large spectral weight only at the surface (interface) layers that decreases exponentially toward the bulk (the bulk and the film). Another indication for a surface or an interface state is that its energy does not change significantly if the number of Ag layers of a comparably thick film is increased. The energy of a QW state, however, will change rather strongly because it is derived from the dispersive Ag *sp* band.

Finally, we briefly address the dependence of the work function on film thickness. The work function for uncovered V(001) (4.56 eV) is drastically increased upon adding 1 ML of Ag (5.72 eV) and drops slightly for 2 ML (5.44 eV). For larger thicknesses, it oscillates around the value for semi-infinite Ag(001) (5.02 eV).

B. Photoelectron spectroscopy

Photoemission intensities were calculated according to the multiple-scattering formulation (the LKKR method) of the one-step model of PES (for details, see Refs. 41 and 42).

For the analysis of QW states, the constant-initial-state (CIS) mode of photoemission is very well suited. In this mode, the fixed initial-state energy is chosen as that of the electronic state of interest while the photon energy is varied. The comparison of theoretical CIS spectra from different QW states may be complicated by the fact that the lifetimes of the quasiparticles (photoelectron and photohole) decrease when moving in energy away from E_F. If large enough, this energy-dependent broadening of the intensity maxima may prevent the observation of trends in the photoemission intensities. This problem can be overcome in theory by deliberately choosing energy-independent lifetimes. Experimental data for Ag/Fe(001) (Ref. 22) proved Fermi-liquid behavior with inverse lifetimes of about 0.027 eV at E_F and about 0.13 eV at -2.0 eV. Hence we derived 0.1 eV as the approximate mean value for the inverse lifetime of the photohole in the *sp*-band range. For the inverse lifetime of the photoelectron we chose 2.0 eV, a reasonable value in the range of kinetic energies up to 35 eV.

In this paper, we are concerned with QW states belonging to the Δ_1 representation. According to the dipole selection rules, these states can be excited only by the component of the electric-field vector $\vec{E}$ of the incoming light that is normal to the surface.[43] Therefore, we have chosen linearly polarized light with $\vec{E} \propto (0,0,1)$. Note that all intensities shown in this paper stem exclusively from QW states because of the dipole selection rules and the Δ_1 band gap in V.

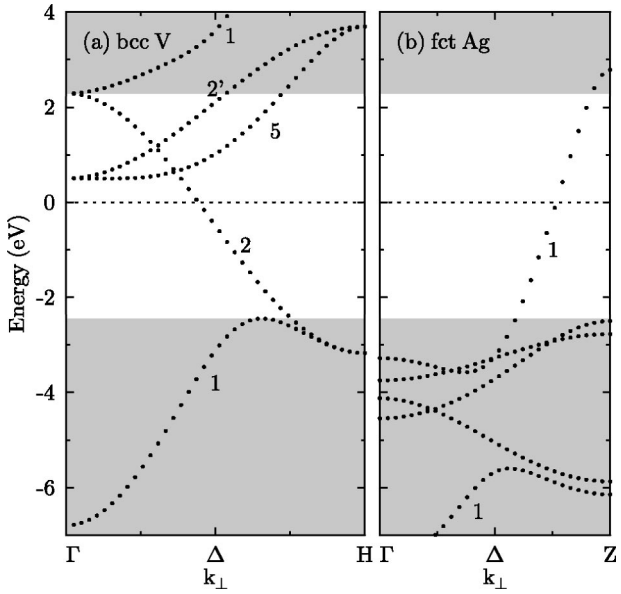

FIG. 2. Bulk-band structures of (a) bcc V and (b) fct Ag for wave vectors along [001] (Δ), i.e., normal to the layers at $\bar{\Gamma}$ ($\vec{k}_\parallel = 0$). Some bands are labeled by their group representation. Gray areas indicate the Δ_1 band gap of V. The Fermi levels are indicated by horizontal dotted lines (at 0 eV).

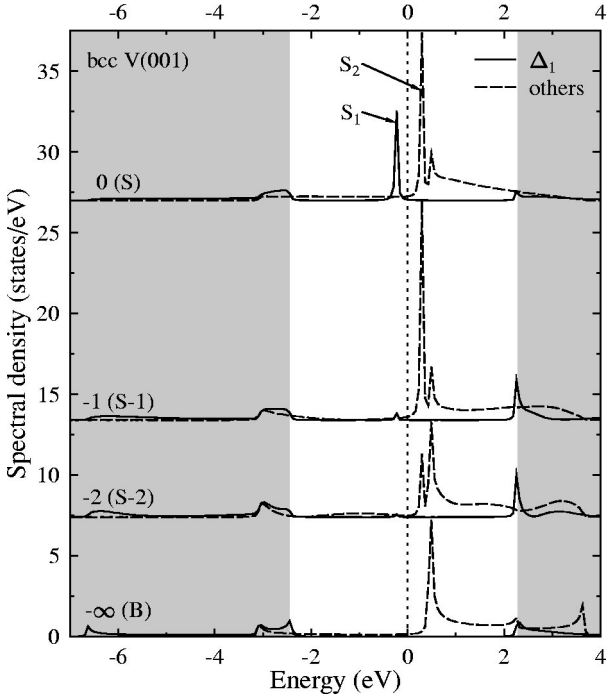

FIG. 3. Electronic structure of the V(001) surface at $\bar{\Gamma}$. The spectral densities of the surface layers 0, -1, and -2, as well as of a bulk layer $-\infty$ (with alternative nomenclature given in brackets), are resolved with respect to the group representation: Δ_1, solid lines, others, dashed lines. S_1 and S_2 denote surface states. Gray areas indicate the Δ_1 band gap of V [cf. Fig. 2(a)]. The Fermi energy is marked by the vertical dotted line.

III. RESULTS AND DISCUSSION

A. Electronic structure

To understand the electronic structures of ultrathin films deposited on a substrate, one has to understand first the respective bulk electronic structures. It is further helpful to investigate some asymptotic cases. The V(001) surface represents the uncovered system. The surface side of a thick fct Ag films leads to the Ag(001) surface as a limiting system, whereas its interface side is represented by an interface between semi-infinite V(001) and fct Ag(001). In other words, we used the theoreticians ''box of bricks'' for achieving detailed informations.

1. Bulk electronic structures

First, we turn to the band structures of bcc V and fct Ag for $\bar{\Gamma}$, that is, along [001] in the bulk ($\vec{k}_\parallel = 0$, the in-plane wave vector relevant for photoemission normal to the surface). The *d* bands of the early TM vanadium are almost completely unoccupied (atomic configuration $3d^3 4s^2$) and therefore lie mostly above the Fermi level E_F [taken as 0 eV; Fig. 2(a)]. Only a Δ_2 band crosses E_F. A gap in the Δ_1 bands extends from -2.45 up to 2.29 eV (cf. the gray areas).

The noble metal Ag has filled *d* bands that lie more than 2.5 eV below E_F (atomic configuration $4d^{10}5s^1$). The Fermi level is crossed by the *sp* band which belongs to the Δ_1 representation [Fig. 2(b)]. Note that all bands of fct Ag show an increased dispersion compared to fcc Ag due to the decreased interlayer distance.

2. Surface electronic structures

Next, the electronic structures of semi-infinite V(001) and fct Ag(001) are briefly addressed, with a focus on the Δ_1 states. For V(001), a strong Δ_1 surface state in layer 0 (labeled *S* in alternative nomenclature) shows up at -0.3 eV (S_1 in Fig. 3). The sensitivity of this surface state to temperature, preparation conditions, and defect concentration was investigated using both conventional PES and inverse PES by Pervan *et al.*[44] (also see Ref. 28). Recent experiments using scanning tunneling spectroscopy confirmed these findings.[45] Further, Valla *et al.* observed a complete destruction of the PES intensity upon adding 1 ML of Ag (see Fig. 3 in Ref. 34). This behavior is consistent with our calculations for Ag/V(001). The strong sensitivity of S_1 to the boundary conditions is corroborated by its spectral weight almost completely located at the outermost vanadium layer 0 (S). In agreement with other theoretical work, a strong peak labeled S_2 occurs 0.3 eV above E_F, with the largest spectral weight in layer -1 ($S-1$). This maximum was considered responsible for the surface being paramagnetic.[24] However, recent theoretical work[25,26] shows that the magnetism of the V surface depends strongly on the assumed interlayer distances and on the choice of the approximation for the exchange-correlation potential (local spin-density approximation, generalized gradient approximation; for a topical review, see Ref. 46). Taking bulk interlayer distances and the local spin-density approximation, we did not find a magnetic surface in a spin-polarized calculation, in accordance with other work.[27]

As the first asymptotic case of very thick Ag films, the surface electronic structure of fct Ag(001) is shown in Fig. 4.

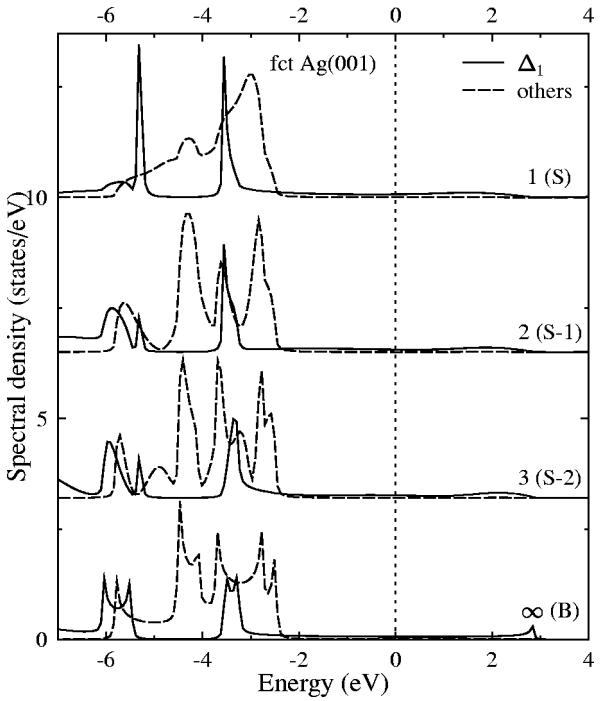

FIG. 4. Same as Fig. 3, but for the fct Ag(001) surface.

In the *d*-band range, there are two distinct Δ_1 maxima at -5.3 and -3.6 eV, respectively, at the outermost surface layer 1 (S). More important for this work is that there are no surface states in the Δ_1 band gap of V. Hence the QW states of thick films (where the influence of the substrate becomes small) are not expected to be ''contaminated'' by surface states.

3. Interface electronic structures

We now focus on an interface between semi-infinite bcc V(001) and fct Ag(001), the second asymptotic case for very thick films. The layer-resolved charge differences $\Delta Q_l = Q_l^{\mathrm{mt}} - Q_l^{\mathrm{at}}$, i.e., the difference of the muffin-tin charge Q_l^{mt} and the atomic charge Q_l^{at} ($23e$ for V, $47e$ for Ag) at layer l, are shown in Fig. 5. The region of charge redistribution extends from V layer -2 to Ag layer 4, i.e., over a range of seven layers. The most pronounced feature is a strong decrease of about 0.2e at the outermost Ag layer 1. This charge is mostly transferred to the adjacent V layers (-1 and 0), each of which shows an increase of about $0.1e$. It is worth mentioning that we find almost identical charge transfers for Ag films of finite thicknesses, except for the 1-ML film. For the latter system, the charge of layer 1 is increased by about $0.3e$, as it is for all surface layers of the thicker films. We would like to mention that the layer-resolved charge profiles can to a good approximation be regarded as superpositions of two individual profiles: that of the Ag(001) surface and that of the V(001)/Ag(001) interface (for superpositions of magnetic-moment and of anisotropy-energy profiles, see Ref. 47). Obviously, these superpositions do not work for films a few ML thick. In summary, the charge redistribution at the interface layers evidences hybridization between V and Ag.

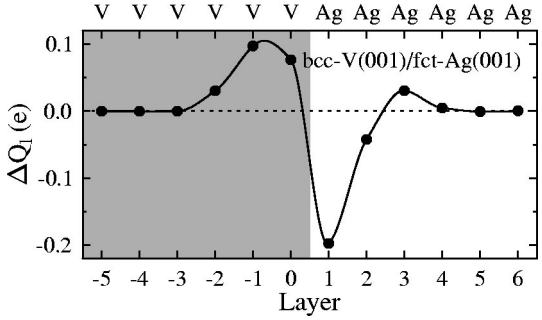

FIG. 5. Charge redistribution at an interface between semi-infinite bcc V(001) and fct Ag(001). The charge differences ΔQ_l (see the text) are plotted vs layer l. The gray area visualizes the V substrate.

A question arises whether the charge transfer has significant influence on the SD at $\bar{\Gamma}$, in particular, concerning Δ_1 states. Therefore, the SD of the V(001)/Ag(001) interface, resolved with respect to group representation and layer, is shown in Fig. 6. Comparing the SD of the V(001) surface with that of the V layers at the V/Ag interface, one observes that the surface state S_1 (Fig. 3) is missing at the interface. Instead one finds a broad distribution of spectral weight within the Δ_1 band gap (black areas at the V layers). This is of course most significant at layer 0 because the associated electronic states are pinned at the interface due to the Δ_1 band gap. A closer analysis reveals that most contributions to this broad distribution stem from *d* states. Hence, we are dealing with a hybridization of Ag *sp* states with V *d* states. This finding is consistent with the enhancement of the effective mass in the $\vec{k}_\parallel$ dispersion of the QW state energies.[34] Finally, the spectral weights of the other group representations do not differ significantly from those at the V(001) surface.

Comparing the SD at the Ag(001) surface [layer 1 (S) in Fig. 4] with that of the Ag layer 1 adjacent to the interface, one finds that the strong maximum at about -3 eV has disappeared. Due to the change of boundary conditions (i.e., the surface barrier is replaced by semi-infinite V), two strong interface states show up at -4.65 and -4.12 eV, respectively. Further, the Δ_1 surface state at -3.6 eV has disappeared and there are no pronounced Ag states within the Δ_1-band gap. These findings are consistent with the charge reduction at this layer as discussed before (note that SD's are $\vec{k}_\parallel$ resolved, whereas charges are $\vec{k}_\parallel$-integrated quantities).

To summarize, we conclude that there is a sizable hybridization between Ag *sp* states and V *d* states, accompanied by a transfer of charge from Ag to V and a transfer of spectral weight from the Ag *d*-band range into the Δ_1 band gap. As we will see in the following, this hybridization has a pronounced effect on the QW states.

4. Quantum-well states

Before discussing the QW states in Ag films on V(001), we first outline a simple picture of QW state formation. The Δ_1 band gap of V prevents the *sp* electrons of Ag in this energy range from penetrating into the V substrate. This spatial confinement results in quantum-well states belonging to

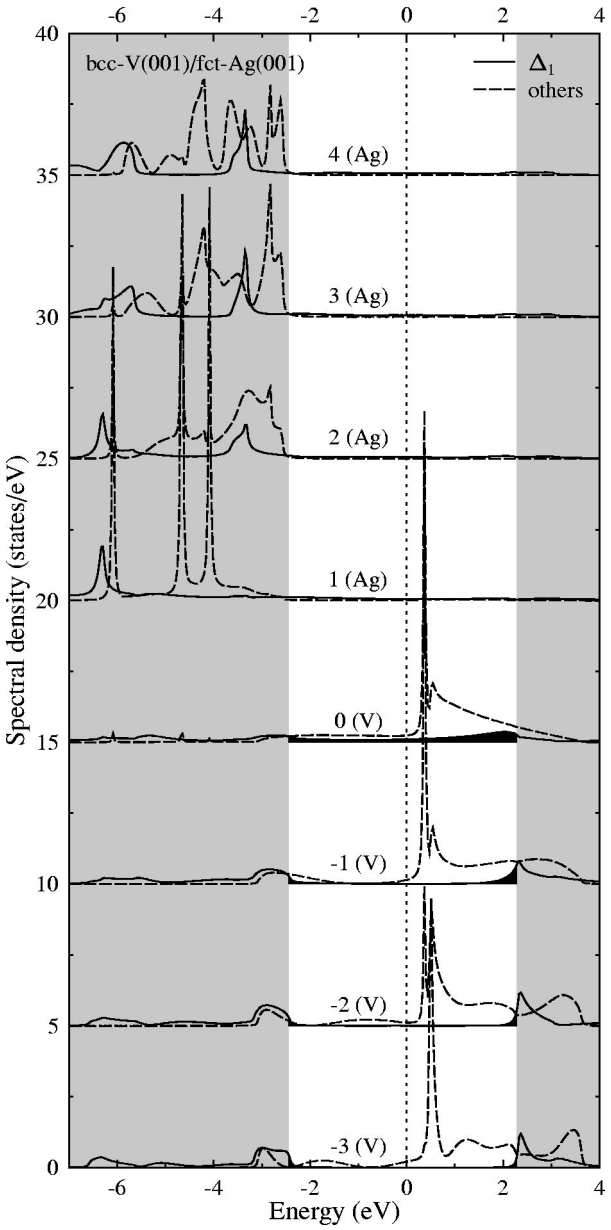

FIG. 6. Electronic structure of an interface between semi-infinite bcc V(001) and fct Ag(001) at $\bar{\Gamma}$. The spectral density of four layers adjacent to the interface (V, bottom, Ag, top; with the layer index given in the middle) is resolved with respect to the group representation: Δ_1, solid lines, others, dashed lines. Gray areas depict the Δ_1-band gap of V [see Fig. 2(a)]. Black areas in the V layers indicate spectral weight in the Δ_1-band gap (see the text). The Fermi energy is given by the vertical dotted line.

the Δ_1 representation. According to the interferometer picture, the occurrence of a QW state requires constructive interference. Hence the phase shift accumulated during a complete round-trip has to obey the so-called round-trip criterion, $\Phi_s+\Phi_i+2\Phi_d=2\pi m$, where m is an integer, and Φ_s and Φ_i are the phase shifts due to reflection at the surface and at the film–substrate interface, respectively. The phase Φ_d is due to propagation from one boundary to the other and can be expressed as $k_\perp N d_0$ (for $\vec{k}_\parallel=0$), where N is the film thickness

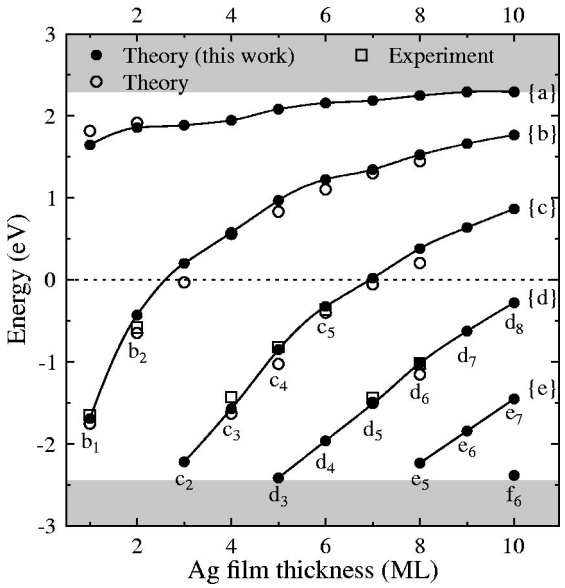

FIG. 7. Energies of quantum-well states (filled circles) at $\bar{\Gamma}$ vs the Ag film thickness. The quantum-well states are labeled according to the nomenclature introduced in Sec. III A 4. Eye-guiding lines connect energies that belong to the same family of QW states ($\{a\}$, $\{b\}$, . . . , as denoted on the right). Gray areas indicate the Δ_1-band gap of the bulk-band structure of V (cf. Fig. 2). Data taken from Ref. 34 are given by empty circles (theory) and squares (experiment). The Fermi energy is given by the dotted line.

(in ML) and d_0 is the interlayer distance. Therefore, each QW state can be labeled by N_m. An alternative nomenclature is obtained by translating N_m into $\aleph(N-m+1)_{m+1}$, where $\aleph(i)$ is the ith lowercase letter of the Latin alphabet.[21,34,48] As an example, quantum-well states 1_0 and 5_2 are named b_1 and d_3, respectively. To be consistent with previous work, the latter nomenclature is used in this paper. Further, we call the set of all QW states with the same letter $\aleph$ a "family" $\{\aleph\}$ (for sketches of the wavefunctions associated with the QW states, see Fig. 2 in Ref. 35).

The energies of QW states versus film thickness are shown in Fig. 7. The dispersion of each family can be regarded as typical since it has been found in other systems as well as in model calculations. The families approach the upper band edge of the Ag sp band (2.78 eV; cf. Fig. 2) with increasing film thickness, but the respective states become resonant with V Δ_1 states, i.e., they lie within the upper gray area. This feature is clearly visible in the layer-resolved spectral densities (see below). The experimental data (empty squares; taken from Ref. 34) agree nicely with our theoretical results. The largest deviation in energy is about 0.1 eV and can, for example, be attributed to the assumed tetragonal distortion in the Ag films. Note that we assumed the fct distortion being independent of the film thickness.

Concerning the dispersion with film thickness, our results agree nicely with other theoretical ones (empty circles in Fig. 7; for details, see Refs. 21 and 34) but lie slightly higher in energy. In particular, QW state b_3 is clearly above E_F, which is in agreement with experiment. Milun and coworkers found a shoulder in the 3-ML photoemission intensities

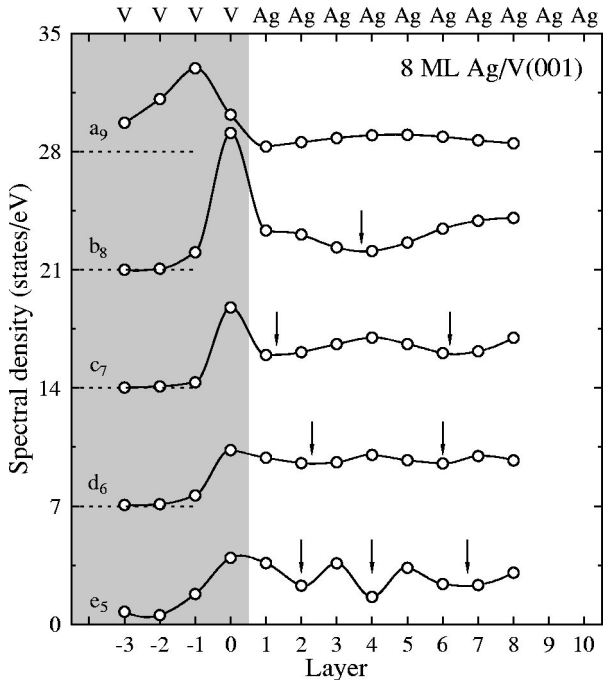

FIG. 8. Oscillatory behavior of quantum-well (QW) states for an 8-ML Ag film on V(001). The layer-resolved spectral densities (the QW state given on the left) at $\bar{\Gamma}$ are shifted for clarity, with the respective abscissae indicated by dotted lines. The gray area visualizes the V substrate layers, arrows mark distinct minima.

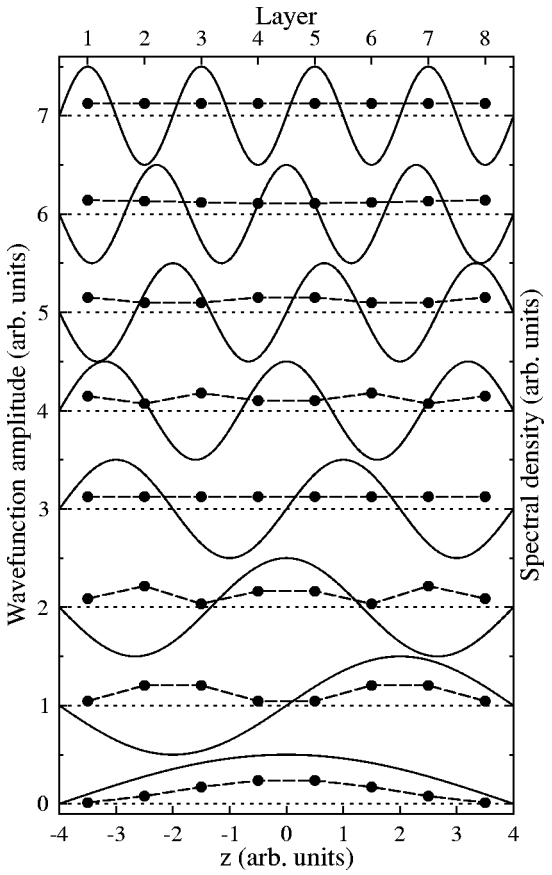

FIG. 9. One-dimensional potential well with infinite barriers and 8-ML width. The wave functions of QW states N_m with $N=8$ and $m=0,\ldots,7$ (as indicated on the left) are represented by solid lines and are evenly shifted for clarity (the respective zero amplitudes are given by dotted lines). The spectral densities are averaged over the individual layers (filled circles; upper abscissa and right ordinate).

that apparently belonged to a maximum above E_F but was cut off by the Fermi-Dirac distribution (cf. Fig. 4 in Ref. 35).

Next, the oscillatory behavior of the QW states at a fixed film thickness is briefly addressed. As an example, consider a Ag film eight layers thick (Fig. 8). The state a_9 at 2.29 eV is almost resonant with the V states and shows minor spectral weight in the Ag film. The strictly confined QW states e_5, d_6, c_7, and b_8 have energies of -2.23, -1.02, 0.38, and 1.53 eV, respectively. Hence, one expects an increasing number of nodes from e_5 $(m=4)$ toward b_8 $(m=7)$. Note that QW states with less nodes cannot show up because there is spatial confinement only at energies within the Δ_1 band gap. It is hardly possible to observe directly the number of nodes in the layer-resolved SD's: In the KKR method, the SD contains averaging over the muffin-tin spheres and, thus, oscillations with wavelengths shorter than 2 ML will show up with an longer effective wavelength. This is easily understood as an aliasing effect due to the discrete sampling. Figure 9 shows wave functions and layer-averaged SD's of QW states of a one-dimensional potential well with hard walls (which can be solved analytically). One clearly sees how the rapid oscillations in the wavefunctions of QW states with a large number of nodes m are obscured due to the discrete presentation in terms of SD's. Therefore, the SD's for Ag/V behave opposite than expected: b_8 shows the least oscillations, e_5 the most (cf. the arrows in Fig. 8). This result is consistent with analytical model calculations for a potential well with infinitely high barriers and N layers of thickness: The layer-averaged SDs of QW states with four, five, and six nodes of a 8-ML QW compare well with those of c_5, d_6, and b_8, with obvious deviations due to the surface and interface. Hence we regard the minima in Fig. 8 as manifestations of the QW states' nodal structures.

Another aspect to be discussed is the confinement of the QW states. For quantum-well states close in energy to the lower boundary of the Δ_1 band gap at -2.56 eV, e.g., d_3, the confinement to the Ag films is rather weak (Fig. 10). This is apparent from comparing the SD at V layers of QW state d_3 with those of the other members of $\{d\}$. The latter show a typical exponential decay towards the V bulk (i.e., a strict confinement to the film), whereas the former shows distinct oscillations in the V layers (i.e., weak confinement). This behavior can be explained by the complex bulk-band structure of V [Figs. 11(a) and 11(b)]. The energetically lower Δ_1 band of V shows a maximum at two-thirds of $\Gamma-\Delta-H$ on the real $k_\perp$-axis [panel (b)]. This $k_\perp$ point is connected by a complex band of the third kind to another extremum in the real band structure at a higher energy (we follow the nomenclature of complex bands introduced by Chang[49]). Therefore, the imaginary part of this complex band increases with energy [panel (a)]. Its real part, however, remains almost constant in a sizable energy range. The corresponding electronic states in V decay toward the bulk [due to the finite $\mathrm{Im}(k_\perp)$]

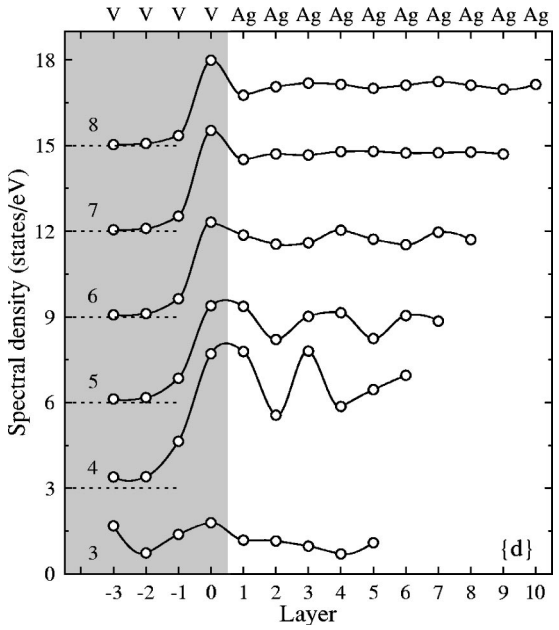

FIG. 10. Confinement of quantum-well (QW) states. The layer-resolved spectral densities of QW state family {d} (as indicated on the left) at $\overline{\Gamma}$ are shifted for clarity, with the respective abscissae indicated by dotted lines. The gray area visualizes the V substrate layers.

but show oscillations [due to the finite Re($k_\perp$)]. Now consider two QW states labeled q_1 and q_2 in Fig. 11(c), with QW state q_1 lying energetically closer to the lower boundary of the Δ_1 band gap. The wave functions of the QW states can be derived in first approximation from the respective bulk states at the relevant energies, i.e., they can be described by

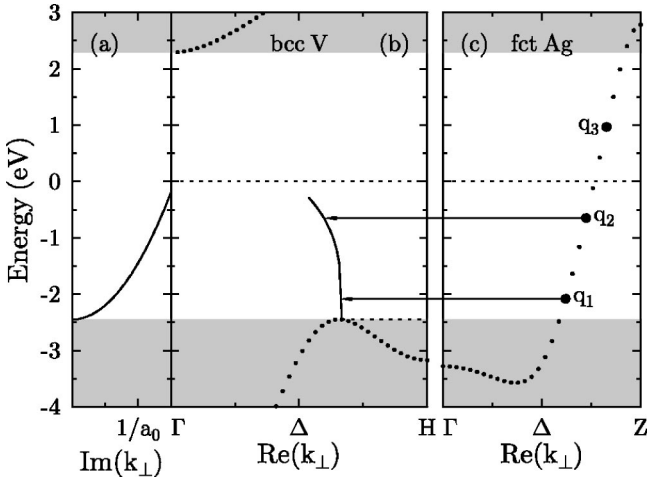

FIG. 11. Scheme of quantum-well (QW) state formation in fct-Ag/V(001) at $\overline{\Gamma}$ ($\vec{k}_\parallel = 0$). The Δ_1 band of Ag (c) gives rise to three QW states (q_1, q_2, and q_3, filled circles) with energies in the Δ_1-band gap of V (gray areas). The Ag band at the energy of QW state q_1 has roughly the same Re($k_\perp$) as the complex V band [schematically depicted in the left panels (a) and (b)]. Further, the small Im($k_\perp$) results in weak confinement of this QW state to the Ag film. Only Δ_1 bands are shown.

the real wavenumber $k_\perp$. Evidently, $k_\perp$ of q_1 is closer to Re($k_\perp$) of the complex V band than $k_\perp$ of q_2. And Im($k_\perp$) is smaller for q_1 than for q_2. Thus the wave function of q_1 is expected to match better to that in the V layers than that of q_2. This explains eventually the weak confinement of q_1 and the more strict confinement of q_2. We note in passing that a similar behavior is found for family $\{a\}$ which becomes resonant with V states with increasing film thickness (cf. a_9 in Fig. 8).

A strong enhancement of the SD at the outermost V layer 0 is present in all families, most pronounced in family $\{b\}$ (cf. b_8 in Fig. 8). As is evident from our considerations for the interface electronic structure, this increase results from the hybridization of Ag-sp with V-d states. Hence the quantum-well states extend about 1–2 ML into the V substrate. Because the Ag-induced spectral weight in layer 0 spans the whole Δ_1 band gap, the enhancement is observed for almost all QW states, an exception being those lying energetically close to the band edges (e.g., d_3 and a_{11}). Note that this enhancement at the interface is missing, for example, in Cu/Co systems.

One could speculate on a possible alloying at the Ag/V interface. Such a disorder effect would significantly change the reflection properties of the interface (in comparison to an abrupt interface) and, according to the round-trip criterion, would result in energy shifts of the QW states. However, the good agreement of the theoretical binding energies with the experimental ones (Fig. 7) suggests that alloying at the interface is rather unlikely.

Summarizing, the energies of the QW states show the typical and expected behavior. However, the layer-resolved SD's reveal considerable band-structure effects and a strong hybridization between Ag and V. Note that, in particular, the latter effect is usually ignored in model calculations and was, for example, not observed in Cu films on Co(001).

B. Photoelectron spectroscopy

1. Quantization effects

Model calculations for photoemission from QW states revealed pronounced ''fingerprints'' of the QW initial states in the spectra: a weakening of the wave vector conservation with decreasing film thickness and pronounced oscillations with film thickness as well as with photon energy.[7] *Ab initio* photoemission calculations for the prototypical system Cu/Co(001) confirmed these results: Oscillations in the CIS spectra from QW states could be directly attributed to the spatial confinement of the initial state.[7,50] In the following analysis, we first focus on spectra within a family of QW states (e.g., family $\{d\}$) in which both binding energy and film thickness vary. Second, for fixed film thickness, we investigate spectra from different QW states. Third, film thickness effects show up in spectra of QW states with almost identical binding energy (e.g., c_3, d_5, and e_7).

It appears helpful to consider as references CIS spectra for semi-infinite fct Ag(001) recorded for the binding energies of the QW states (dashed lines in Fig. 12). Concentrating on family $\{d\}$, one notices a striking similarity to spectra for Cu(001) (see Fig. 7 in Ref. 7), not too surprising a coin-

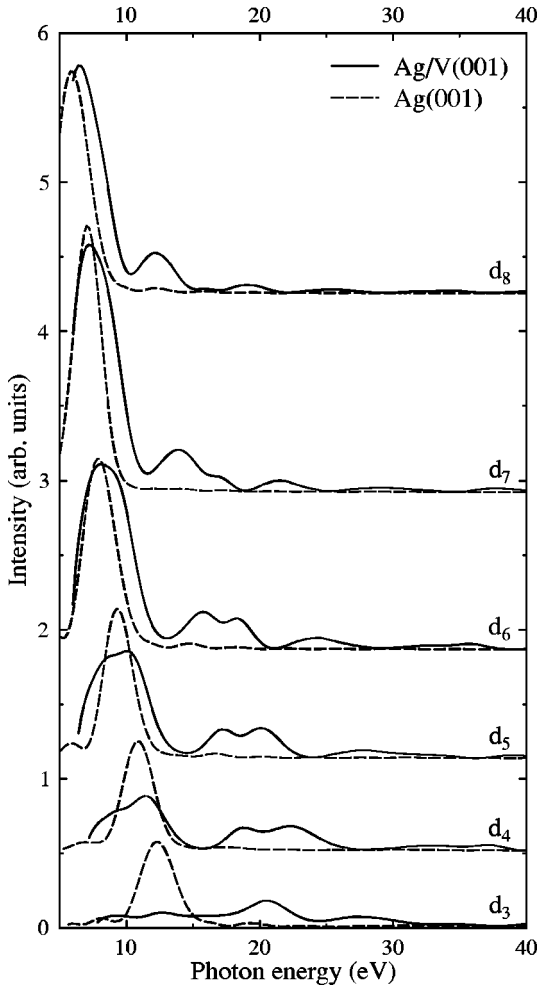

FIG. 12. Photoemission from quantum-well (QW) state family $\{d\}$ at $\bar{\Gamma}$ ($\vec{k}_{\parallel}=0$). The intensity of the constant-initial-state spectra (solid lines; as indicated on the right of each spectrum) is plotted vs the photon energy. Spectra for semi-infinite Ag(001) with initial energy of the respective QW states are shown in addition (dashed). The incoming light is linearly polarized with the electric-field vector normal to the surface.

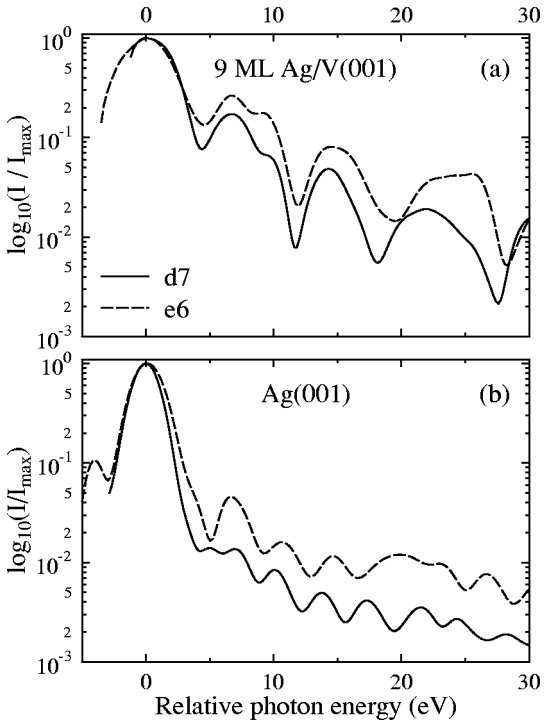

FIG. 13. Constant-initial-state photoemission from quantum-well (QW) states in 9-ML Ag/V(001) at $\bar{\Gamma}$. (a) Spectra for QW states e_6 and d_7. (b) Spectra for semi-infinite Ag(001) with corresponding initial energies. The data normalized to maximum intensity ($I_{\max}$) are shifted in energy to obtain coincident maxima (''relative photon energy'').

cidence since Cu and Ag are isoelectronic. Further, a pronounced maximum at 12.3 eV photon energy for d_3 disperses down to 6.0 eV for d_8. This maximum is due to a direct transition from the sp-band into the ''free-electron-like'' final-state band. The largest intensity occurs in spectra for initial-state energies of about -0.6 eV (cf. d_7, with an initial energy of -0.62 eV). Comparing the dispersion with experimental data (e.g., Fig. 8 in Ref. 35), the maxima in experiment occur at slightly higher photon energies than their theoretical counterparts. This shift is also observed in other systems and can be attributed to the real part of the photoelectron's self-energy (a decrease of the real part of the inner potential with kinetic energy). Besides the main maximum, much smaller maxima show up due to excitations into other final states.

Quantum-well states allow a for band-structure determination (''band mapping''),[48,51] if the main maximum in the CIS spectra for a film occurs at the same photon energy as in the spectra for the semi-infinite system. This was proven again by model calculations as well as by photoemission calculations for Cu/Co(001).[7] For Ag/V(001), the sharp maximum of the QW state d_8 at 6.4 eV coincides rather well with that of semi-infinite Ag(001) (Fig. 12). With decreasing film thickness, and hence decreasing initial-state energy, this main maximum disperses to higher photon energies, but the agreement with Ag(001) gets worse. The most striking example is d_3, for which the main maximum is missing. This QW state is almost resonant with V states and shows a comparably weakly structured SD (Fig. 10). For states d_4 to d_6, the main maximum appears to be made up of two structures. This ''separation'' into two peaks was already observed for Cu/Co(001), and could clearly be attributed to quantization effects. The two subpeaks merge in the limit of infinite film thickness, as is corroborated by inspection of the d_8 spectrum. However, even for a 10-ML film, the main maximum is slightly broader than its counterpart for semi-infinite Ag(001).

Further insight can be gained by considering spectra from QW states at a particular film thickness. Here we choose the strictly confined QW states e_6 and d_7 in the 9-ML film (Fig. 13). Using a logarithmic scale, the intensity oscillations become clearly visible: the spectra show distinct minima at about the same energy. Deviations occur at energies larger than 17 eV. Comparing the spectra with corresponding ones for semi-infinite Ag(001), one notices a significantly sharper main maximum (at 0 eV) and a shorter period of the oscil-

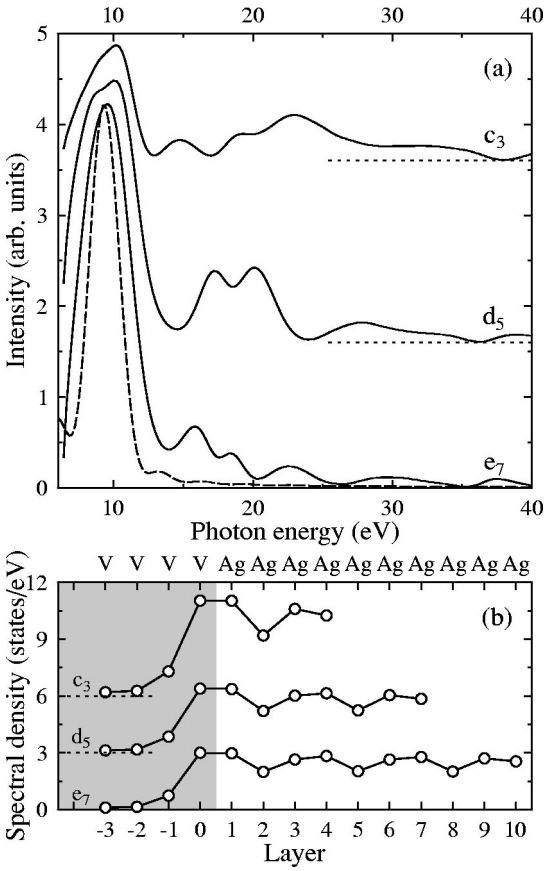

FIG. 14. Constant-initial-state photoemission from quantum-well states c_3, d_5, and e_7 at $\bar{\Gamma}$ (a). A spectrum for semi-infinite Ag(001) with an initial energy of e_7 is shown in addition (dashed). Dotted lines indicate the respective zero intensity. The spectral densities of the initial states are shown in addition (b).

lations. Further, the intensity drops much faster with (relative) photon energy than for the Ag film. These findings agree nicely with those for Cu/Co(001) and can therefore be regarded as typical quantum-size effects.

To investigate the effect of increasing $k_\perp$ conservation with film thickness, we consider QW states with almost identical binding energy: c_3 (4 ML), d_5 (7 ML), and e_7 (10 ML). The spectral profiles are very similar and display a regular pattern of 3-ML wavelength, in particular minima at layers 2, 5, and 8 [Fig. 14(b) (the expected numbers of nodes of the wave functions are 2, 4, and 6; the layer-averaged SDs of corresponding QW states in an infinitely high potential well are in good accord with those in Fig. 14(b)]. Considering the photoemission intensities [Fig. 14(a)], the main intensity maxima occur at almost identical photon energies for all QW states (9.6 eV) and grow considerably when going from c_3 to e_7. The spatial confinement of the electrons manifests itself in two features. First, the width of the main maximum decreases with film thickness. In the limit of very thick films, its width is obtained from the spectrum for semi-infinite Ag(001) [dashed in Fig. 14(a)]. Second, the wavelengths of the intensity oscillations with photon energy decrease with film thickness. In conclusion, we observe significant fingerprints of quantization effects. However, trends in the spectra are not as pronounced as for the prototypical system Cu/Co(001) (see Fig. 8 in Ref. 7).

To summarize, we find pronounced manifestations of quantum-size effects in the CIS spectra for strictly confined QW states. Obvious exceptions are almost resonant states (e.g., d_3), the spectra of which differ significantly from those of the confined states (as was shown for Cu/Co(001), QW resonances can be distinguished from QW states by their pattern of intensity oscillations[7]). With respect to prototypical systems, such as Cu/Co(001) and Ag/Fe(001), the trends in the spectra with film thickness and energy are not as clear.

2. Comparison with experiment

Milun *et al.* concluded from their very elaborate experimental study[35] (accompanied by model photoemission calculations) that ''the idea that *all* QW state photoemission should peak in intensity at the conditions appropriate for a direct transition in the bulk film material at the same initial state binding energy is not correct'' (emphasis by the authors). In particular, they found intensity minima in photoemission from the film where photoemission from semi-infinite Ag(001) produced a maximum. On the one hand, our theoretical study corroborates the above statement. For example, in the CIS spectrum for d_7 a significant minimum at about 18 eV coincides with a maximum in the corresponding spectrum from Ag(001) (Fig. 13). On the other hand, we find that the main maxima in photoemission from Ag(001), which are due to transitions into the ''free-electron'' final-state band, coincide with distinct maxima in photoemission from the Ag films (Fig. 12). Further, both systems show the same trend regarding the maximum intensity. Unfortunately, the main maxima occur at photon energies (below 14 eV) that are not covered in Ref. 35.

Since Figs. 12–14 reveal significant differences in the spectra for Ag/V(001) and Ag(001) regarding the intensity structures at higher photon energies, it appears interesting to compare our theoretical results with experimental ones (Fig. 15). As mentioned earlier (Sec. II B), we did not optimize the free parameters in theory and, thus, a very good agreement with experiment cannot be expected. Further, there are indications that the Ag films do not grow as perfectly (roughness, islands),[35] as assumed in theory. The structures of corresponding spectra as well as trends should, however, be reproduced. As becomes evident on inspection of Fig. 15, the global shape of the theoretical spectra agrees rather well with that in experiment (cf. in particular b_2, c_3, and c_5). However, at certain photon energies significant differences occur. For example, d_5 displays a maximum at 23 eV (arrow in Fig. 15) and a minimum at 26 eV in experiment, whereas theory shows the opposite behavior. A further obvious exception is b_1 for the 1-ML film which in theory shows a maximum at 19 eV which is missing in experiment.

To conclude, the comparison of theory with experiment[35] corroborates the statement quoted before—at least for structures other than the main intensity maxima. However, to draw a final conclusion, we suggest performing experiments which cover lower photon energies to address the main intensity maxima. Further, uncertainties in both experiment (e.g., roughness, islands) and theory (e.g., values chosen for

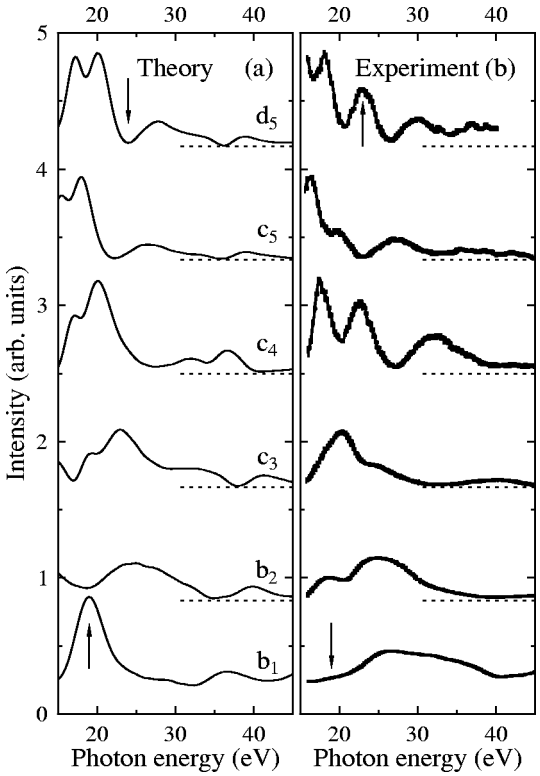

FIG. 15. Constant-initial-state photoemission from quantum-well states: (a) theory and (b) experiment (reproduced from Ref. 35). Dotted lines indicate zero intensities, and arrows mark features discussed in the text.

free parameters) should be overcome. Finally, it would be helpful to consider film systems made-up of early transition metals other than V.

IV. CONCLUDING REMARKS

Model calculations for the formation of quantum-well states utilize either a rectangular potential well or an atomic chain of finite length, both of which show sharp boundaries.[52] The substrate is either completely neglected or taken into account in a simple manner. This results in a strong localization of the quantum-well states which manifests itself in pronounced and regular oscillations of the wavefunction modulus. The prototypical systems Cu/fcc-Co(001) and Ag/Fe(001) apparently fit nicely into this class of systems and, thus, the measured photoemission intensities display prominent oscillations with film thickness and photon energy. Both exhibit clear and pronounced trends in the spectra.

As evidenced by this work and recent experimental investigations,[34–36] Ag/V(001) shows a twofold behavior. On the one hand, the energies of the quantum-well states agree nicely with those expected from model calculations and the main intensity maxima of the constant-initial-state photoemission spectra ''follow'' the bulk bands. On the other hand, Ag/V(001) has a comparably ''soft'' boundary at the Ag/V interface due to hybridization. Therefore, the wavefunctions of the quantum-well states extend about 1–2 layers into the substrate. These salient features are reflected by the photoemission spectra which, for instance, show much less pronounced trends [as compared to Cu/Co(001)] and show in some cases minor maxima (minima) where minor minima (maxima) are expected.

In conclusion, Ag films on V(001) reveal the limits of model calculations,[11] in particular with regard to the influence of the substrate. To understand the properties of these systems, first-principles calculations in conjunction with photoemission calculations are necessary. We hope that this work will encourage further experimental investigations on quantum-well states in early transition-metal systems.

ACKNOWLEDGMENTS

We are grateful to Phil Woodruff (Coventry), Milorad Milun (Zagreb), and Börje Johansson (Uppsala) for pointing us to this interesting systems as well as for fruitful and clarifying discussions. This work was supported by the EU through the RTN ''Computational Magnetoelectronics'' (HPRN-CT-2000-00143).

*Corresponding author. Electronic address: henk@mpi-halle.de

[1] P. Bruno, J. Magn. Magn. Mater. **148**, 202 (1995).
[2] A.M.N. Niklasson, L. Nordström, S. Mirbt, B. Johansson, and H. Skriver, J. Phys.: Condens. Matter **11**, 975 (1999).
[3] S. Mirbt, H.L. Skriver, and B. Johansson, Phys. Rev. B **53**, R13 310 (1996).
[4] A.M.N. Niklasson, S. Mirbt, H.L. Skriver, and B. Johansson, Phys. Rev. B **56**, 3276 (1997).
[5] J.E. Ortega, F.J. Himpsel, G.J. Mankey, and R.F. Willis, Phys. Rev. B **47**, 1540 (1993).
[6] M. Grüne, T. Pelzer, K. Wandelt, and I.T. Steinberger, J. Electron Spectrosc. Relat. Phenom. **98–99**, 121 (1999).
[7] J. Henk and B. Johansson, J. Electron Spectrosc. Relat. Phenom. **105**, 187 (1999).
[8] A. Shik, *Quantum Wells* (World Scientific, Singapore, 1997).
[9] P. Harrison, *Quantum Wells, Wires and Dots* (Wiley, Chichester, 2000).
[10] T.-C. Chiang, Surf. Sci. Rep. **39**, 181 (2000).
[11] M. Milun, P. Pervan, and D.P. Woodruff, Rep. Prog. Phys. **65**, 99 (2002).
[12] A. Carlsson, D. Claesson, S.-Å. Lindgren, and L. Walldén, Phys. Rev. B **52**, 11 144 (1995).
[13] A. Carlsson, D. Claesson, G. Katrich, S.-Å. Lindgren, and L. Walldén, Surf. Sci. **352–354**, 656 (1996).
[14] R.K. Kawakami, E. Rotenberg, H.J. Choi, E. Escorcia-Aparicio, M.O. Bowen, J.H. Wolfe, E. Arenholz, Z.D. Zhang, N.V. Smith, and Z.Q. Qiu, Nature (London) **398**, 132 (1999).
[15] A. Mugarza, J.E. Ortega, A. Mascaraque, E.G. Michel, K.N. Altmann, and F.J. Himpsel, Phys. Rev. B **62**, 12 672 (2000).
[16] C. Carbone, E. Vescovo, O. Rader, W. Gudat, and W. Eberhardt, Phys. Rev. Lett. **71**, 2805 (1993).
[17] C. Carbone, E. Vescovo, R. Kläsges, D. Sarma, and W. Eberhardt, Solid State Commun. **100**, 749 (1996).
[18] P. van Gelderen, S. Crampin, and J. Inglesfield, Phys. Rev. B **53**, 9115 (1996).

[19] P. Segovia, E.G. Michel, and J.E. Ortega, Phys. Rev. Lett. **77**, 3455 (1996).
[20] E.D. Hansen, T. Miller, and T.-C. Chiang, J. Phys.: Condens. Matter **9**, L435 (1997).
[21] N.V. Smith, N.B. Brookes, Y. Chang, and P.D. Johnson, Phys. Rev. B **49**, 332 (1994).
[22] J.J. Paggel, T. Miller, and T.-C. Chiang, Science **283**, 1709 (1999).
[23] J.J. Paggel, T. Miller, and T.-C. Chiang, J. Electron Spectrosc. Relat. Phenom. **101–103**, 271 (1999).
[24] S. Ohnishi, C.L. Fu, and A.J. Freeman, J. Magn. Magn. Mater. **50**, 161 (1985).
[25] I.G. Batyrev, J.-H. Cho, and L. Kleinman, Phys. Rev. B **63**, 172420 (2001).
[26] R. Robles, J. Izquierdo, A. Vega, and L.C. Balbás, Phys. Rev. B **63**, 172406 (2001).
[27] G. Bihlmayer, T. Asada, and S. Blügel, Phys. Rev. B **62**, R11 937 (2000).
[28] P. Pervan, T. Valla, and M. Milun, Solid State Commun. **89**, 917 (1994).
[29] I. Turek, S. Blügel, and J. Kudrnovský, Phys. Rev. B **57**, R11 065 (1998).
[30] T. Valla, M. Kralj, A. Siber, M. Milun, P. Pervan, P.D. Johnson, and D.P. Woodruff, J. Phys.: Condens. Matter **12**, L477 (2000).
[31] M. Stampanoni, A. Vaterlaus, D. Pescia, M. Aeschlimann, F. Meier, W. Dürr, and S. Blügel, Phys. Rev. B **37**, 10 380 (1988).
[32] R.L. Fink, C.A. Ballentine, J.L. Erskine, and J.A. Araya-Pochet, Phys. Rev. B **41**, 10 175 (1990).
[33] F. Wilhelm, P. Poulopoulos, H. Wende, A. Scherz, K. Baberschke, M. Angelakeris, N.K. Flevaris, and A. Rogalev, Phys. Rev. Lett. **87**, 207202 (2001).
[34] T. Valla, P. Pervan, M. Milun, A.B. Hayden, and D.P. Woodruff, Phys. Rev. B **54**, 11 786 (1996).
[35] M. Milun, P. Pervan, B. Gumhalter, and D.P. Woodruff, Phys. Rev. B **59**, 5170 (1999).
[36] D.P. Woodruff, M. Milun, and P. Pervan, J. Phys.: Condens. Matter **11**, L105 (1999).
[37] U. von Barth and L. Hedin, J. Phys. C **5**, 1629 (1972).
[38] J.P. Perdew and Y. Wang, Phys. Rev. B **45**, 13 244 (1992).
[39] A. Ernst, G. van der Laan, W.M. Temmerman, S.S. Dhesi, and Z. Szotek, Phys. Rev. B **62**, 9543 (2000).
[40] A. Ernst, M. Lüders, W.M. Temmerman, Z. Szotek, and G. van der Laan, J. Phys.: Condens. Matter **12**, 5599 (2000).
[41] J. Braun, Rep. Prog. Phys. **59**, 1267 (1996).
[42] M. Lüders, A. Ernst, W.M. Temmerman, Z. Szotek, and P.J. Durham, J. Phys.: Condens. Matter **13**, 8587 (2001).
[43] J. Hermanson, Solid State Commun. **22**, 9 (1977).
[44] P. Pervan, T. Valla, M. Milun, A.B. Hayden, and D.P. Woodruff, J. Phys.: Condens. Matter **8**, 4195 (1996).
[45] M.M.J. Bischoff, C. Konvicka, A.J. Quinn, M. Schmid, J. Redinger, R. Podloucky, P. Varga, and H. van Kempen, Phys. Rev. Lett. **86**, 2396 (2001).
[46] H. Dreyssé and C. Demangeat, Surf. Sci. Rep. **28**, 65 (1997).
[47] J. Henk, A.M.N. Niklasson, and B. Johansson, Phys. Rev. B **59**, 9332 (1999).
[48] S.Å. Lindgren and L. Walldén, Phys. Rev. Lett. **61**, 2894 (1988).
[49] Y.-C. Chang, Phys. Rev. B **25**, 605 (1982).
[50] A. Mugarza, J.E. Ortega, A. Mascaraque, E.G. Michel, K.N. Altmann, and F.J. Himpsel, Surf. Sci. **482–485**, 464 (2001).
[51] P.D. Loly and J.B. Pendry, J. Phys. C **16**, 423 (1983).
[52] J. Henk, in *Handbook of Thin Film Materials*, edited by H.S. Nalwa (Academic Press, San Diego, 2001), Vol. 2, Chap. 10, p. 479.